Title

Upregulation of cholesterol 24-hydroxylase following hypoxia-ischemia in neonatal mouse brain.

Journal
Pediatric research, 83(6)

ISSN
0031-3998

Authors
Lu, Fuxin
Zhu, Jun
Guo, Selena
et al.

Publication Date
2018-06-01

DOI
10.1038/pr.2018.49

Peer reviewed

Pediatric RESEARCH

Up-regulation of cholesterol 24-hydroxylase following hypoxia-ischemia in neonatal mouse brain

Journal:	*Pediatric Research*
Manuscript ID	PR-2017-0725
Manuscript Type:	Original research article, basic science
Date Submitted by the Author:	13-Nov-2017
Complete List of Authors:	Lu, Fuxin; University of California San Francisco, Pediatrics Zhu, Jun; University of California San Francisco, Laboratory Medicine Guo, Selena; Dougherty Valley High School Chehab, Farid; University of California San Francisco, Laboratory Medicine Ferriero, Donna; Pediatrics Jiang, Xiangning ; University of California San Francisco, Pediatrics;
Keywords:	Brain injury, Hypoxia-ischemia, Neurodevelopment, Oxidative Stress, Biomarkers
Free Text Keywords:	Cholesterol

Up-regulation of cholesterol 24-hydroxylase following hypoxia-ischemia in neonatal mouse brain

Running title: cholesterol metabolism in neonatal brain

Fuxin Lu[1], Jun Zhu[2], Selena Guo[3], Farid F. Chehab[2], Donna M. Ferriero[1,4] and Xiangning Jiang[1*]

Departments of [1]Pediatrics, [2]Laboratory Medicine, [4]Neurology,
University of California San Francisco, San Francisco, CA, USA
[3]Dougherty Valley High School, San Ramon, CA, USA

*** Corresponding author:** Xiangning Jiang, Department of Pediatrics, University of California, San Francisco 675 Nelson Rising Lane Room 494, San Francisco, CA 94158 Phone: 415-502-7278 Fax: 415-502-7325 Email: xiangning.jiang@ucsf.edu

Statement of financial support: This work was supported by the National Institute of Neurological Disorders and Stroke (RO1NS084057 to Dr. Jiang).

Disclosure: The authors have no conflicts of interest and no financial relationships relevant to this article to disclose.

Category of study: basic science

Abstract

Background: Maintenance of cholesterol homeostasis is crucial for brain development. Brain cholesterol relies on de novo synthesis and is cleared primarily by conversion to 24S-hydroxycholesterol (24S-HC) with brain-specific cholesterol 24-hydroxylase (CYP46A1). This study was undertaken to investigate the impact of hypoxia-ischemia (HI) on brain cholesterol metabolism in the neonatal mice.

Methods: Postnatal day 9 C56BL/6 pups were subjected to HI using the Vannucci model. CYP46A1 expression was assessed by western blotting and its cellular localization was determined by immunofluorescence staining. The amount of cholesterol and 24S-HC in the cortex and in the serum was measured with ELISA.

Results: There was a transient cholesterol loss at 6hr after HI. CYP46A1 was significantly up-regulated at 6hr and 24hr following HI with a concomitant increase of 24S-HC in the ipsilateral cortex and in the serum. The serum levels of 24S-HC correlated with those in the brain, as well as with necrotic and apoptotic cell death evaluated by the expression of spectrin breakdown products and cleaved-caspase 3 at 6hr and 24hr.

Conclusions: Enhanced cholesterol turnover by activation of CYP46A1 represents disrupted brain cholesterol homeostasis early after neonatal HI. 24S-HC might be a novel blood biomarker for severity of hypoxic-ischemic encephalopathy with potential clinical application.

Introduction

Human brain cholesterol, which constitutes 25% of total body cholesterol, is crucial for brain development due to its importance in membrane integrity, myelination, synaptogenesis and neurotransmission (1, 2). Brain cholesterol is stored primarily in myelin sheaths, and the rest in the membranes of neurons, glial cells and other cellular elements. To accommodate rapid brain growth in the neonatal period, the rates of cholesterol biosynthesis and accretion are the greatest during this stage (first 3 weeks after birth in the rodents), a critical time for neuroplasticity, and decline with age to reach a constant cholesterol level in the adulthood (3-6). Cholesterol biosynthesis is unique in the brain because it is produced exclusively from de novo synthesis (3, 7) using Acetyl-CoA as starting material and HMG-CoA reductase (HMGCR) as the rate-limiting enzyme. Cholesterol carried in lipoproteins in the blood cannot cross the blood brain barrier (BBB), however, its metabolite 24S-hydroxycholesterol (24S-HC) through hydroxylation by cholesterol 24-hydroxylase (CYP46A1), is capable of traversing BBB and entering circulation to the liver for excretion (4, 7). CYP46A1 is brain-specific (4, 8), thus most circulating 24S-HC has a cerebral origin (9) and the serum 24S-HC level could be an indication of brain cholesterol metabolism (10). In fact, plasma 24S-HC has been used as a surrogate marker of neuronal loss and brain atrophy in neurodegenerative diseases such as Alzheimer disease, Parkinson's disease and multiple sclerosis (11).

Cholesterol biosynthesis involves multiple enzymatic reactions and is an oxygen-consumptive process that requires 11 oxygen molecules for the conversion of Acetyl-CoA to cholesterol (12). Therefore, cholesterol synthesis is sensitive to reduced O_2 availability and is limited in the conditions of hypoxia-ischemia (HI). This was evidenced by two studies in neonatal HI rats showing chronic loss of brain cholesterol lasting at least 3 days or 3 months following the insults

(13, 14). Unfortunately, there are no additional investigations on the changes of cholesterol metabolism in response to HI in the immature brain and the underlying mechanisms. Recent in vitro studies suggested that oxidative stress (6) and endogenous neurotransmitters upregulate CYP46A1, with glutamate eliciting the highest increase in CYP46A1 activity (15). These are well-accepted mechanisms that are associated with brain damage in neonatal hypoxic-ischemic encephalopathy (HIE), the clinical syndrome of brain dysfunction in the newborns with few tools for diagnosis and intervention (16). Studies on regulation of cholesterol homeostasis in the developing brain, as well as its disturbance after HI at early postnatal stage would allow for a better understanding of lipid disorders and their involvement in HIE gray and white matter injury.

The present study focused on the responses of cholesterol metabolism after neonatal HI in postnatal day 9 (P9) mice, an age equivalent to full term human infants. We hypothesized that the brain-specific cholesterol hydroxylase, CYP46A1, is activated following neonatal HI leading to enhanced production of 24S-HC in the brain, and in the circulation. Herein, we demonstrated an increase and correlation of the 24S-HC levels in the serum and in the brain, and importantly, a significant positive correlation between serum 24S-HC levels and cortical injury evaluated by the expression of spectrin breakdown products (SBDPs) and cleaved caspase-3, representing activation of necrosis and/or apoptosis, at 6hr and 24hr after HI. These findings suggested a possibility of using 24S-HC as a potential blood biomarker for severity of HIE brain injury.

Methods

All animal experiments were approved by the University of California San Francisco institutional animal care and use committee. C57BL/6 mice (Charles River Laboratory, Hollister, CA) with litters were allowed food and water *ad libitum*. Both sexes were used at P9.

Neonatal Brain Hypoxia-Ischemia

Neonatal HI was performed using the Vannucci model. At P9, the pups underwent left common carotid artery coagulation through a vertical midline neck incision under isoflurane anesthesia (2-3% isoflurane, balanced oxygen) to induce unilateral ischemia. The animals were recovered for one hour with their dam and then exposed to 60 minutes of hypoxia in a humidified chamber at 37°C with 10% oxygen/balanced nitrogen to induce global hypoxia. Sham-operated control animals received isoflurane anesthesia and exposure of the left common carotid artery without coagulation and hypoxia. HI and sham animals were dissected immediately after hypoxia (0hr) or were returned to their dams until they were euthanized at 1hr, 6hr, 24hr, 48hr and 72hr after the procedure for different experiments.

Sample preparation

The cortices were dissected and quickly sliced into small pieces on ice, mixed and divided into 3 equal fractions for protein, or lipid extraction for western blotting, cholesterol or 24S-HC measurements respectively. For protein purification, the tissue was homogenized in radioimmunoprecipitation assay (RIPA) buffer (R0278, MilliporeSigma, Temecula, CA) with protease and phosphatase inhibitors followed by centrifugation at 14,000 rpm for 15mins. The supernatant was saved and the protein concentration was measured with BCA kit (Pierce Biotechnology, Rockford, IL). For 24S-HC assay, the tissue was sonicated with 95% ethanol, after centrifugation at 7,000 ×g for 5mins, the supernatant (A) was collected and the pellet was sonicated again in the extract buffer (ethanol: dichloromethane (1:1; v/v)) followed by centrifugation at 7,000 ×g for 5 mins. The resultant supernatant (B) was combined with supernatant A and dried with speed vacuum. The dried pellet was rehydrated by adding 8µl of 95% ethanol and 242µl of assay buffer 40 (24S-Hydroxycholesterol ELISA Kit, ab204530, Abcam, Cambridge, MA). For cholesterol measurement, the tissue was extracted with 200µl of chloroform: isopropanol: IGEPAL CA-630 (7:11:0.1) in a microhomogenizer and spinned at 13,000 × g for 10 mins to remove insoluble material. The organic phase was air-dried at 50• for 15 mins to remove chloroform. The samples were then dried with speed vacuum for 30 mins and dissolved in 200µl cholesterol assay buffer (Cholesterol Quantitation Kit, MAK043, MilliporeSigma) for cholesterol quantification.

Serum was collected from the same animals using BD SST microtainer capillary blood collection tube with serum separator (#365967, BD, Franklin Lakes, NJ).

Western blotting

For Western blot analysis, an equal amount of protein samples (40µg) was applied to 4-12% Bis-Tris SDS polyacrylamide gel electrophoresis and transferred to polyvinylidene difluoride (PVDF) membrane at 30V overnight at 4^{o}C. After blocking with TBS containing 0.05% Tween 20 (TBST) buffer with 5% milk for 1 hour, the blots were probed overnight at 4°C with the following primary antibodies: anti-cholesterol-24-hydroxylase 1A7 (1:500; MAB2259, MilliporeSigma); anti-α-spectrin (1:5000, MAB1622, MilliporeSigma); anti-cleaved-caspase 3 (1:1000, # 9664, Cell Signaling Technology Inc.; 3 Trask Lane, Danvers, MA) and anti-β-actin (1:5000, sc-47778, Santa Cruz Biotechnology Inc., Santa Cruz, CA). Appropriate secondary HRP-conjugated antibodies (Santa Cruz Biotechnology Inc.) were used. The protein signal was visualized with enhanced chemiluminescence and developed with radiographic film. Image J software was used to measure the mean optical densities (OD) and areas of protein signal on the film after scanning.

Enzyme-linked immunosorbent assay for 24S-HC levels in the cortex and serum

A competitive ELISA kit (ab204530, Abcam) was used to measure the levels of 24S-HC in the cortical tissue and serum. A fresh set of 24S-HC standard were prepared at a range of 0.39ng/ml to100ng/ml. A clear 96 well plate coated with goat anti-rabbit IgG was used for the analysis. Briefly, 100µl of standards and samples were pipetted into the appropriate wells. 50µl of the diluted biotin-labeled 24S-HC conjugate was then added to each well except for the blanks. 50µl of the rabbit 24S-HC antibody that can bind to either 24S-HC in the samples or the labeled 24S-HC conjugate was added to each well except for the blanks and the nonspecific binding (NSB) wells. The plate was incubated for 1 hour at RT. After washing for 4 times with 400µl of wash buffer, 200µl of streptavidin-HRP solution was pipetted into each well to bind to biotin-labeled 24S-HC conjugate. The plate was incubated for 30 mins at RT. After the 2nd wash, 200µl of 3,3',5,5'-Tetramethylbenzidine (TMB) substrate solution was added and the plate was incubated at RT for 30 mins without shaking. To stop the reaction, 50µl of stop solution (1N HCl) was added to each well. The absorbance (optical density, OD) was read at 450nm with a microplate reader (BioTek Synergy HT). The intensity of signal is inversely proportional to the level of 24S-HC in the samples. For each standard and sample, the net OD = OD-NSB OD. A standard curve was made for the calculation of the levels of 24S-HC. The concentration of cortical 24S-HC was normalized to the wet weight of the starting tissue (ng/mg wet weight). The concentration of serum 24S-HC was normalized to the serum protein concentration (ng/mg protein).

Cholesterol measurement

A cholesterol quantitation kit (MAK043, MilliporeSigma) was used to measure the concentration of cholesterol in the cortical samples. The samples prepared above were diluted at 1:10 with assay buffer and 7 cholesterol standards (0.02 µg/µl to 0.14 µg/µl) were prepared. 100µl of standards and samples were pipetted into the appropriate wells of a clear 96 well plate.

50µl of reaction mix buffer including cholesterol probe, cholesterol enzyme mix and cholesterol esterase was add to each well. The plate was incubated at 37°C for 60 mins protected from light. The absorbance was read at 570nm and the concentration of cholesterol in the samples was calculated using the standard curve. The levels of cortical cholesterol were normalized to the wet weight of the starting tissue (µg/mg wet weight).

Immunofluorescent staining

Sham-operated mice and the mice at 24hr after the HI procedure were perfuse-fixed with 4% paraformaldehyde (PFA) in 0.1mol/L phosphate buffer (pH 7.4). Brains were dissected and post-fixed in 4% PFA overnight at 4□C, and then transferred to 30% sucrose in 0.1mol/L phosphate buffer for cryoprotection for 3 days. The brains were embedded in O.C.T compound and cryosections were cut at 16µm. The sections were defrosted and air-dried at RT for 2 hrs. After washing with PBS for 10 mins, sections were boiled in 0.01M sodium citrate buffer (pH 6.0, with 0.05% Tween 20) at 90°C for 30 mins to retrieve antigen. After washing with PBS for 5 mins, the sections were blocked with blocking buffer (10% goat serum and 0.1% Triton X-100 in PBS) for 1 hr and then incubated overnight at 4°C with mouse anti-CYP46A1 antibody (1:50, MAB2259, MilliporeSigma), or paired with another rabbit antibody that labels different cell types: anti-NeuN for neurons (1:500, #ab177487, Abcam); or anti-GFAP for astrocytes (1:500, #Z0334, Dako, Santa Clara, CA); or anti-Iba1 for microglia (1:1000, #019-19741, Wako Chemicals, Richmond, VA); or anti-MBP for oligodendrocytes (1:200, #78896, Cell Signaling Technology). After washing with 0.025% Tween/PBS for 3 times, the sections were incubated with goat anti-mouse Alexa Fluor 568 (1:500; # A-11004, Invitrogen, Grand Island, NY) and goat anti-rabbit Alexa Fluor 488 (1:500, #A-11034, Invitrogen) for 1hr at RT and exposed to

DAPI for 5 min and then cover-slipped with ProLong Diamond antifade reagent (Invitrogen). Images were taken with Leica TCS SP5 Spectral Confocal Microscope.

Statistical Analysis

SAS Wilcoxon-Mann-Whitney test was used to evaluate the OD values of protein expression in Western blotting, brain concentrations of cholesterol, and the cortical and serum levels of 24S-HC. Pearson's correlation coefficient analysis was used to evaluate the correlation between cortical and serum levels of 24S-HC, and between serum 24S-HC and protein levels of spectrin breakdown product (SBDP) at 145/150KDa, SBDP120KDa, or cleaved-caspase 3. Differences were considered significant at $p<0.05$.

Results

Up-regulation of CYP46A1 with a concomitant increase of 24S-HC in the brain following neonatal HI

To investigate how cholesterol metabolism is impacted by neonatal HI, we measured the protein expression of CYP46A1, the enzyme responsible for elimination of excess cholesterol from the brain, at various post-HI time points for up to 3 days. As shown in Fig.1A, CYP46A1 was significantly upregulated at 6hr and 24hr after HI compared to the sham animals at the same time points, and declined at 48hr and 72hr (sham vs. HI: p= 0.0339 at 6hr; p=0.0026 at 24hr; n=5-6 for sham animals, n=6-12 for HI animals at 6-72hr). The increased expression of CYP46A1 was confirmed by immunofluorescent staining with anti-CYP46A1 antibody, where the fluorescent intensity was much higher in the ipsilateral cortex compared to the sham animals and the contralateral hemisphere at 24hr after HI (Fig.1B).

The pattern of 24S-HC levels in the ipsilateral cortex was similar to that of CYP46A1 expression with a marked increase at 6 and 24hr post-HI compared to the sham controls (Fig. 1C, sham vs. HI: p= 0.0167 at 6hr; p=0.0085 at 24hr; n=3-6 for sham animals, n=5-7 for HI animals at 6-72hr). At 6hr, 24S-HC in the ipsilateral cortex was higher than that in the contralateral side, too (Fig. 1C, ipsi vs. contra: p=0.0493 at 6hr). HI-induced over-production of 24S-HC in the ipsi-cortex sustained at 48hr although the difference was not statistically significant compared to the sham animals (Fig. 1C, sham vs. HI: p=0.0526 at 48hr). There was a trend of more 24S-HC produced in the contralateral cortex (underwent hypoxia) at 6 and 24hr, but the differences were not significant (Fig. 1C, right panel). These results demonstrated that the up-regulated CYP46A1 was functional, which led to robust cholesterol turnover early after HI, along with an enhanced production of its metabolic product 24S-HC in the injured cortex, but not in the non-injured contralateral hemisphere.

To determine whether the increased cholesterol metabolism following neonatal HI would diminish cholesterol amount, we measured cholesterol levels in the sham and HI-injured ipsi- and contra-lateral cortex at the same time points. We found a significant, but transient loss of cholesterol at 6hr after HI in the ipsilateral cortex (Fig. 2A, sham vs. HI: p=0.0304 at 6hr; n=7), but not in the contralateral side (sham vs. HI contra: p=0.1736; n=7) compared to the sham animals. This data represent the net results of de novo cholesterol synthesis and turnover. The enhanced cholesterol hydroxylation/breakdown may, at least in part, contribute to the cholesterol loss at 6hr, while the elevated expression of HMGCR, the rate-limiting enzyme for cholesterol biosynthesis, at 24hr (Fig. 2B, 2C, sham vs. HI: p=0.047 at 24hr, n=4-11) indicates feedback mechanisms for replenishment and re-establishment of cholesterol balance at 24hr and the time points thereafter.

Expression of CYP46A1 in neurons and oligodendrocytes

CYP46A1 was originally reported to be neuron-specific, however, several recent studies demonstrated its presence in glial cells, including microglia and astrocytes in different injury paradigms (17, 18). To study the cellular localization of CYP46A1 in our neonatal HI model, we stained the brain sections from the sham and injured pups (at 24hr post-HI) with CYP46A1 antibody paired with another antibody specific for neuron (NeuN), astrocyte (GFAP), oligodendrocyte (MBP) or microglia (Iba1). Fig. 3 indicated that the enzyme was expressed in neurons (shown in the cortical region) and oligodendrocytes (OLGs, shown in the corpus callosum) in both sham (Fig. 3A) and the injured animals (Fig. 3B). Co-localization was not found in the astrocytes and microglia in the sham (not shown) and injured brains (Fig. 3B). The CYP46A1 staining was in the cytoplasm.

Correlation of the 24S-HC levels in the serum and in the brain after neonatal HI

As CYP46A1 converts brain cholesterol to the more soluble 24S-HC, which readily crosses BBB, and this enzymatically-generated oxysterol is specifically made in the brain, we asked whether there is an efflux of 24S-HC from the brain into the periphery circulation after HI. We measured the serum levels of 24S-HC and evaluated its relationship with brain levels. In line with the increased production in the brain, there was a boost of serum 24S-HC levels at 6hr after HI, which maintained elevated for 48hr before returning to the sham values at 72hr (Fig. 4A, sham vs. HI, p=0.0102 at 6hr; p=0.0046 at 24hr; p=0.0167 at 48hr; n=4-6 for sham animals, n=5-13 for HI animals at 6-72hr). There was a strong correlation of 24S-HC levels in the serum and in the ipsilateral cortex (Fig. 4B, R^2=0.521, p< 0.0001, n = 40) implicating brain as the major source of circulating 24S-HC (note that the concentrations of 24S-HC in the serum was normalized to serum protein concentration as ng/mg protein, while in the brain it was normalized to the tissue wet weight as ng/mg wet weight).

Correlation of serum 24S-HC levels with brain injury at 6hr and 24hr after HI

Since cholesterol is essential for membrane and myelin integrity, CYP46A1 upregulation may cause membrane disruption or myelin breakdown leading to cell death and brain injury after HI, we hypothesized that increased serum 24S-HC values could forecast HI-induced cell loss and gray/white matter damage. We assessed acute brain injury within 3 days with the protein expression of spectrin breakdown products (SBDP) at 145/150 KD and 120KD representing activation of necrosis and/or apoptosis , as well as the cleaved-caspase 3 indicating apoptotic cell death . The expression of SBDP at 145/150KD and 120KD both considerably increased at 6hr and 24hr after HI compared to the sham animals (Fig. 5A, for SBDP145/150KD, sham vs. HI, $p=0.0094$ at 6hr, $p=0.0013$ at 24hr. For SBDP120KD, sham vs. HI, $p=0.036$ at 6hr, $p=0.0087$ at 24hr. n=4-6 for sham animals, n=6-15 for HI animals from 6-72hr). The increase in cleaved-caspase 3 levels lasted longer for 48hrs and subsided at 72hr (Fig. 6A, sham vs. HI, $p=0.0112$ at 6hr; $p=0.0027$ at 24hr; $p=0.0228$ at 72hr, n=5-6 for sham animals, n=7-10 for HI animals from 6-72hr). There was a positive correlation of serum 24S-HC levels with SBDP 145/150KD at 6hr and 24hr post-HI (Fig. 5B, at 6hr: $R^2=0.713$, $p=0.002$, n=10; at 24hr: $R^2=0.656$, $p=0.003$, n=11); and with cleaved-caspase-3 at the same time points (Fig. 6B, at 6hr: $R^2=0.738$, $p=0.002$, n=10; at 24hr: $R^2=0.462$, $p=0.044$, n=9). The correlation of serum 24S-HC with SBDP120 kD was also significant at 24hr (Fig. 5B, $R^2=0.557$, $p=0.008$, n=11).

Discussion

We demonstrated an enhanced brain cholesterol turnover following neonatal hypoxia-ischemia as evident by the up-regulation of CYP46A1 in the ipsilateral cortex, leading to an increased production of 24S-HC in the injured hemisphere and simultaneous excretion into the bloodstream. The levels of serum 24S-HC correlate with brain necrosis/apoptosis at early post-HI stage supports a possible value of plasma level of 24S-HC as a novel and early biomarker for severity of neonatal HI brain damage.

Present mainly in the brain, CYP46A1 catalyzes the hydroxylation of cholesterol into 24S-HC to eliminate surplus cholesterol from the brain, and thereby plays an important role in maintenance of cholesterol homeostasis (19, 20). CYP46A1 protein expression is low before 1 week after birth in mouse and gradually increases to reach a steady level around 3 weeks (6, 8). In human it reaches adult level around 3 years old (8). This allows deposition of nearly all cholesterol at early age to assist rapid expansion of brain and myelin, and removal of redundant cholesterol as the animal matures. We showed an upregulation of CYP46A1 following neonatal HI at P9 sustaining at least 24 or 48hrs. It is unknown how this enzyme is activated by hypoxia-ischemia, whether this response is simply adaptative, or is involved in processes of brain injury or protection. CYP46A1 promoter activity appears to be resistant to changes of molecules implicated in regulation of cholesterol homeostasis including cholesterol and 24S-HC (6), but can be induced by the Sp-family of transcriptional factors (21) and epigenetic modifications (22). Recent studies have suggested two mechanisms for CYP46A1 activation: oxidative stress (6) and glutamate (15), both of which are associated with cell death in brain ischemia, and with overactivation of the NMDA receptors (NMDARs), the major ionotropic glutamate receptors mediating excitotoxicity in HI brain injury. CYP46A1 enzymatic product 24S-HC was found to be a potent allosteric modulator to enhance the function of NMDARs (23, 24). These findings suggest a reciprocal activation of the NMDAR pathway and the cholesterol metabolism pathway, which may form a viscous cycle to exacerbate brain damage following neonatal HI.

Cholesterol loss is expected to be the direct consequence of CYP46A1 activation. This might be partially responsible for the reduction in cholesterol in the ipsilateral cortex at 6hr after HI. The total cholesterol amount measured here reflected the balance between de novo synthesis and breakdown by CYP46A1. We did not measure cholesterol that is newly synthesized after neonatal HI, however, elevated generation of 24S-HC could down-regulate cholesterol synthesis via blocking the proteolytic activation of transcription factor sterol regulatory element-binding protein 2 (SREBP2), which controls pathway of cholesterol biosynthesis (25). In connection with excitotoxicity, a Ca^{2+}-dependent cholesterol loss was found in cultured hippocampal neurons exposed to NMDA, which was paralleled by translocation of CYP46A1 from the endoplasmic reticulum, where it normally resides, to the plasma membrane and release of 24S-HC into the medium (26). Apparently, we cannot draw the conclusion that cholesterol loss at 6hr is solely attributable to the action of CYP46A1. The level of HMGCR was unchanged at 6hr, but increased at 24hr after HI, which might prevent further reduction of cholesterol in the injured hemisphere. The other two studies of neonatal HI in P7 SD rats also reported the diminished cholesterol contents, but lasted longer for 3 days or 3 months following the initial insult (13, 14). Disturbance of cholesterol homeostasis after neonatal HI may have adverse consequences on cell survival and brain development, for example, accelerated cholesterol hydroxylation found in this study produced high dose of 24S-HC, which has been shown to be cytotoxic to neurons by inducing apoptosis, necroptosis (a form of programmed necrosis) (27, 28), inflammatory responses (29) and cognitive impairment (30). Further studies are required to elucidate the functional roles of CYP46A1 and 24S-HC in neonatal HI, especially in long-term neurological deficits.

Although primarily confined to neurons in the healthy brain, CYP46A1 has been found in other cell types in different disease conditions, for example, in activated microglia and reactive astrocytes in brain trauma (17, 18), in astrocytes of Alzheimer disease patients (31), or in macrophages/microglia in an animal model of multiple sclerosis (32). They were proposed to clear extracellular cholesterol released from damaged cell membranes, which has not been proved experimentally. We show that CYP46A1 is localized in neurons and oligodendrocytes, but not in astrocytes and microglia. White matter is a common lesion site in rodent neonatal HI (33), and in human infants suffered from HIE, especially in preterm birth (34). As oligodendrocytes are sensitive to oxidative stress and excitotoxicity in the developing brain (35), CYP46A1 in oligodendrocytes after HI may break down cholesterol leading to myelin degradation or limiting its availability for myelin synthesis and whiter matter development as cholesterol in oligodendrocytes is a rate-limiting factor for brain maturation (2). Targeted inhibition or deletion of CYP46A1 in oligodendrocyte may reveal its precise function in normal brain and in disease conditions. Neurons can utilize external cholesterol transported from glial cells (36, 37), similarly, different cell populations may have distinct function, but coordinate intercellularly for cholesterol clearance because not all brain cells; even not all neurons, express CYP46A1 (8, 20).

Studies with CYP46A1 knockout mice have suggested that this enzyme is responsible for the production of ≈ 98-99% of brain 24S-HC and ≈ 60-80% 24S-HC in the serum (9, 38). Our data support the cerebral origin of blood 24S-HC owing to the concomitant increase and correlation of 24S-HC in the serum and in the brain. Although it is unknown whether an acute elevation of serum 24S-HC can predict histological and functional outcomes at later times, based on brain specificity, and a strong correlation with necrotic and apoptotic cell death early after HI, this pilot work indicates that blood 24S-HC might be a biologically plausible marker for HIE to assist clinical diagnosis. SBDP can be detected in the serum of human neonates and the amounts are associated with the severity of HIE clinical syndromes with good sensitivity and specificity (39). However, serum SBDP can result from extracerebral organs when damaged. Radiological or functional measures are needed to explore the feasibility of using blood 24S-HC as diagnostic tool in HIE patients. Targeted lipid profiling discovered plasma sphingomyelins as potential markers for acute stroke patients (40). Lipids could be better tools for diagnosis than protein markers due to their abundance in the brain, small size for readily crossing the BBB, and higher sensitivity to oxidative stress for a possible earlier detection.

Taken together, this is the first study investigating a brain-specific cholesterol turnover pathway following neonatal hypoxia-ischemia. Activation of CYP46A1 may play more specialized roles than just removing cholesterol from the central nervous system. Future work is required to gain better insight into cholesterol homeostasis in the developing brain, which is subject to a more sophisticated regulation than that in the adult brain where cholesterol is largely metabolically inert.

References:

1. Mauch DH, Nagler K, Schumacher S, Goritz C, Muller EC, Otto A, Pfrieger FW 2001 CNS synaptogenesis promoted by glia-derived cholesterol. Science 294:1354-1357.
2. Saher G, Brugger B, Lappe-Siefke C, Mobius W, Tozawa R, Wehr MC, Wieland F, Ishibashi S, Nave KA 2005 High cholesterol level is essential for myelin membrane growth. Nat Neurosci 8:468-475.
3. Dietschy JM 2009 Central nervous system: cholesterol turnover, brain development and neurodegeneration. Biol Chem 390:287-293.
4. Dietschy JM, Turley SD 2004 Thematic review series: brain Lipids. Cholesterol metabolism in the central nervous system during early development and in the mature animal. J Lipid Res 45:1375-1397.
5. Quan G, Xie C, Dietschy JM, Turley SD 2003 Ontogenesis and regulation of cholesterol metabolism in the central nervous system of the mouse. Brain Res Dev Brain Res 146:87-98.
6. Ohyama Y, Meaney S, Heverin M, Ekstrom L, Brafman A, Shafir M, Andersson U, Olin M, Eggertsen G, Diczfalusy U, Feinstein E, Bjorkhem I 2006 Studies on the transcriptional regulation of cholesterol 24-hydroxylase (CYP46A1): marked insensitivity toward different regulatory axes. J Biol Chem 281:3810-3820.
7. Jurevics H, Morell P 1995 Cholesterol for synthesis of myelin is made locally, not imported into brain. J Neurochem 64:895-901.
8. Lund EG, Guileyardo JM, Russell DW 1999 cDNA cloning of cholesterol 24-hydroxylase, a mediator of cholesterol homeostasis in the brain. Proc Natl Acad Sci U S A 96:7238-7243.
9. Bjorkhem I, Lutjohann D, Diczfalusy U, Stahle L, Ahlborg G, Wahren J 1998 Cholesterol homeostasis in human brain: turnover of 24S-hydroxycholesterol and evidence for a cerebral origin of most of this oxysterol in the circulation. J Lipid Res 39:1594-1600.
10. Lutjohann D, von Bergmann K 2003 24S-hydroxycholesterol: a marker of brain cholesterol metabolism. Pharmacopsychiatry 36 Suppl 2:S102-106.
11. Leoni V, Caccia C 2013 24S-hydroxycholesterol in plasma: a marker of cholesterol turnover in neurodegenerative diseases. Biochimie 95:595-612.
12. DeBose-Boyd RA 2008 Feedback regulation of cholesterol synthesis: sterol-accelerated ubiquitination and degradation of HMG CoA reductase. Cell Res 18:609-621.
13. Ramirez MR, Muraro F, Zylbersztejn DS, Abel CR, Arteni NS, Lavinsky D, Netto CA, Trindade VM 2003 Neonatal hypoxia-ischemia reduces ganglioside, phospholipid and cholesterol contents in the rat hippocampus. Neurosci Res 46:339-347.
14. Yu Z, Li S, Lv SH, Piao H, Zhang YH, Zhang YM, Ma H, Zhang J, Sun CK, Li AP 2009 Hypoxia-ischemia brain damage disrupts brain cholesterol homeostasis in neonatal rats. Neuropediatrics 40:179-185.
15. Mast N, Anderson KW, Johnson KM, Phan TTN, Guengerich FP, Pikuleva IA 2017 In vitro cytochrome P450 46A1 (CYP46A1) activation by neuroactive compounds. J Biol Chem 292:12934-12946.
16. Millar LJ, Shi L, Hoerder-Suabedissen A, Molnar Z 2017 Neonatal Hypoxia Ischaemia: Mechanisms, Models, and Therapeutic Challenges. Front Cell Neurosci 11:78.

17. Cartagena CM, Ahmed F, Burns MP, Pajoohesh-Ganji A, Pak DT, Faden AI, Rebeck GW 2008 Cortical injury increases cholesterol 24S hydroxylase (Cyp46) levels in the rat brain. J Neurotrauma 25:1087-1098.
18. Smiljanic K, Lavrnja I, Mladenovic Djordjevic A, Ruzdijic S, Stojiljkovic M, Pekovic S, Kanazir S 2010 Brain injury induces cholesterol 24-hydroxylase (Cyp46) expression in glial cells in a time-dependent manner. Histochem Cell Biol 134:159-169.
19. Moutinho M, Nunes MJ, Rodrigues E 2016 Cholesterol 24-hydroxylase: Brain cholesterol metabolism and beyond. Biochim Biophys Acta 1861:1911-1920.
20. Russell DW, Halford RW, Ramirez DM, Shah R, Kotti T 2009 Cholesterol 24-hydroxylase: an enzyme of cholesterol turnover in the brain. Annu Rev Biochem 78:1017-1040.
21. Milagre I, Nunes MJ, Gama MJ, Silva RF, Pascussi JM, Lechner MC, Rodrigues E 2008 Transcriptional regulation of the human CYP46A1 brain-specific expression by Sp transcription factors. J Neurochem 106:835-849.
22. Shafaati M, O'Driscoll R, Bjorkhem I, Meaney S 2009 Transcriptional regulation of cholesterol 24-hydroxylase by histone deacetylase inhibitors. Biochem Biophys Res Commun 378:689-694.
23. Linsenbardt AJ, Taylor A, Emnett CM, Doherty JJ, Krishnan K, Covey DF, Paul SM, Zorumski CF, Mennerick S 2014 Different oxysterols have opposing actions at N-methyl-D-aspartate receptors. Neuropharmacology 85:232-242.
24. Paul SM, Doherty JJ, Robichaud AJ, Belfort GM, Chow BY, Hammond RS, Crawford DC, Linsenbardt AJ, Shu HJ, Izumi Y, Mennerick SJ, Zorumski CF 2013 The major brain cholesterol metabolite 24(S)-hydroxycholesterol is a potent allosteric modulator of N-methyl-D-aspartate receptors. J Neurosci 33:17290-17300.
25. Radhakrishnan A, Ikeda Y, Kwon HJ, Brown MS, Goldstein JL 2007 Sterol-regulated transport of SREBPs from endoplasmic reticulum to Golgi: oxysterols block transport by binding to Insig. Proc Natl Acad Sci U S A 104:6511-6518.
26. Sodero AO, Vriens J, Ghosh D, Stegner D, Brachet A, Pallotto M, Sassoe-Pognetto M, Brouwers JF, Helms JB, Nieswandt B, Voets T, Dotti CG 2012 Cholesterol loss during glutamate-mediated excitotoxicity. EMBO J 31:1764-1773.
27. Noguchi N, Urano Y, Takabe W, Saito Y 2015 New aspects of 24(S)-hydroxycholesterol in modulating neuronal cell death. Free Radic Biol Med 87:366-372.
28. Yamanaka K, Saito Y, Yamamori T, Urano Y, Noguchi N 2011 24(S)-hydroxycholesterol induces neuronal cell death through necroptosis, a form of programmed necrosis. J Biol Chem 286:24666-24673.
29. Alexandrov P, Cui JG, Zhao Y, Lukiw WJ 2005 24S-hydroxycholesterol induces inflammatory gene expression in primary human neural cells. Neuroreport 16:909-913.
30. Zhao S, Liao W, Xu N, Xu H, Yu C, Liu X, Li C 2009 Polar metabolite of cholesterol induces rat cognitive dysfunctions. Neuroscience 164:398-403.
31. Brown J, 3rd, Theisler C, Silberman S, Magnuson D, Gottardi-Littell N, Lee JM, Yager D, Crowley J, Sambamurti K, Rahman MM, Reiss AB, Eckman CB, Wolozin B 2004 Differential expression of cholesterol hydroxylases in Alzheimer's disease. J Biol Chem 279:34674-34681.
32. Lavrnja I, Smiljanic K, Savic D, Mladenovic-Djordjevic A, Tesovic K, Kanazir S, Pekovic S 2017 Expression profiles of cholesterol metabolism-related genes are altered

during development of experimental autoimmune encephalomyelitis in the rat spinal cord. Sci Rep 7:2702.

33. Liu Y, Silverstein FS, Skoff R, Barks JD 2002 Hypoxic-ischemic oligodendroglial injury in neonatal rat brain. Pediatr Res 51:25-33.
34. Back SA 2017 White matter injury in the preterm infant: pathology and mechanisms. Acta Neuropathol.
35. Silbereis JC, Huang EJ, Back SA, Rowitch DH 2010 Towards improved animal models of neonatal white matter injury associated with cerebral palsy. Dis Model Mech 3:678-688.
36. Funfschilling U, Jockusch WJ, Sivakumar N, Mobius W, Corthals K, Li S, Quintes S, Kim Y, Schaap IA, Rhee JS, Nave KA, Saher G 2012 Critical time window of neuronal cholesterol synthesis during neurite outgrowth. J Neurosci 32:7632-7645.
37. Pfrieger FW, Ungerer N 2011 Cholesterol metabolism in neurons and astrocytes. Prog Lipid Res 50:357-371.
38. Lund EG, Xie C, Kotti T, Turley SD, Dietschy JM, Russell DW 2003 Knockout of the cholesterol 24-hydroxylase gene in mice reveals a brain-specific mechanism of cholesterol turnover. J Biol Chem 278:22980-22988.
39. Wu H, Li Z, Yang X, Liu J, Wang W, Liu G 2017 SBDPs and Tau proteins for diagnosis and hypothermia therapy in neonatal hypoxic ischemic encephalopathy. Exp Ther Med 13:225-229.
40. Sheth SA, Iavarone AT, Liebeskind DS, Won SJ, Swanson RA 2015 Targeted Lipid Profiling Discovers Plasma Biomarkers of Acute Brain Injury. PLoS One 10:e0129735.

Figure Legends:

Figure 1: Up-regulation of CYP46A1 with a concomitant increase of 24S-HC in the ipsilateral cortex after neonatal HI. **A.** Protein expression of CYP46A1 in the sham-operated and HI-injured cortices was measured by western blotting at the indicated time points and presented as the OD ratio to β-actin and normalized to the values of sham 0hr (graph on the right, sham vs. HI: * p= 0.0339 at 6hr; * p=0.0026 at 24hr; n=5-6 for sham animals, n=6-12 for HI animals at 6-72hr). **B.** Immunofluorescent staining with anti-CYP46A1 antibody at 24hr after HI showed enhanced expression in the ipsilateral cortex than that in the contralateral side and in the sham animals. **C.** Increased production of 24S-HC (ng/mg tissue wet weight) in the ipsilateral cortex at 6hr and 24hr after HI (sham vs. HI: *p= 0.0167 at 6hr; *p=0.0085 at 24hr; n=3-6 for sham animals, n=5-7 for HI animals at 6-72hr). The time course of the changes in 24S-HC in the sham-, contra- and ipsilateral cortex is shown on the right. At 6hr, 24S-HC in the ipsilateral cortex was higher than that in the contralateral side (ipsi- vs. contra-: *p=0.0493). #: Significant difference between the ipsi- and the sham animals only, but not between the ipsi- and contralateral hemisphere.

Figure 2: Transient cholesterol loss at 6hr after neonatal HI. **A.** The time course of the changes in cholesterol amount in the sham-, contra- and ipsilateral cortex following neonatal HI (sham vs. HI: * p=0.0304 at 6hr; n=4-7 for each time points). **B.** Protein expression of HMGCR in the sham and HI-injured cortices was measured by western blotting at the indicated time points. **C.** HMGCR expression is presented as the OD ratio to β-actin and normalized to the values of sham 0hr (sham vs. HI: *p=0.047 at 24hr, n=4-11).

Figure 3: Expression of CYP46A1 in the neurons and oligodendrocytes. Images of double Immunofluorescent staining with CYP46A1 antibody (red, middle panels) paired with another

antibody specific for neuron (NeuN), oligodendrocyte (MBP), astrocyte (GFAP), or microglia (Iba1), shown in green on the left panels. The representative images from the sham (**A**) and HI-injured animals at 24hr after HI (**B**).

Figure 4: Correlation of the 24S-HC levels in the serum and in the ipsilateral cortex after neonatal HI. **A.** Quantification of the serum levels of 24S-HC (ng/mg serum protein) at the indicated post-HI time points. Sham vs. HI, *p=0.0102 at 6hr; *p=0.0046 at 24hr; *p=0.0167 at 48hr; n=4-6 for sham animals, n=5-13 for HI animals at 6-72hr. **B.** Correlation of 24S-HC levels in the serum and in the ipsilateral cortex. The samples used in Pearson's correlation coefficient analysis were those included in Fig. 1C. (n = 40, R^2=0.521, p< 0.0001).

Figure 5: Correlation of the serum levels of 24S-HC with the expression of spectrin breakdown products (SBDP) at 6hr and 24hr after neonatal HI. **A.** Protein expression of SBDP145/150KD and SBDP120KD in the sham and HI-injured cortices was measured by western blotting at the indicated time points and presented as the OD ratio to β-actin and normalized to the values of sham 0hr (for SBDP145/150), or an internal control (IC, for SBDP120). For SBDP145/150KD, sham vs. HI, *p=0.0094 at 6hr, *p=0.0013 at 24hr. For SBDP120KD, sham vs. HI, *p=0.036 at 6hr, *p=0.0087 at 24hr. (n=4-6 for sham animals, n=6-15 for HI animals from 6-72hr). **B.** Correlation of serum 24S-HC with the expression of SBDP145/150KD at 6hr (top), at 24hr (middle), and with the expression of SBDP120KD at 24hr (bottom). Sample number, R^2 and p values are shown in the graphs.

Figure 6: Correlation of the serum levels of 24S-HC with the expression of cleaved caspase-3 at 6hr and 24hr after neonatal HI. **A.** Protein expression of cleaved caspase-3 in the sham and HI-injured cortices was measured by western blotting at the indicated time points and presented as the OD ratio to β-actin and normalized to an internal control (IC). Sham vs. HI, *p=0.0112 at

6hr; *p=0.0027 at 24hr; *p=0.0228 at 72hr (n=5-6 for sham animals, n=7-10 for HI animals from 6-72hr). **B.** Correlation of serum 24S-HC with the expression of cleaved caspase-3 at 6hr (top) and at 24hr (bottom). Sample number, R^2 and p values are shown in the graphs.

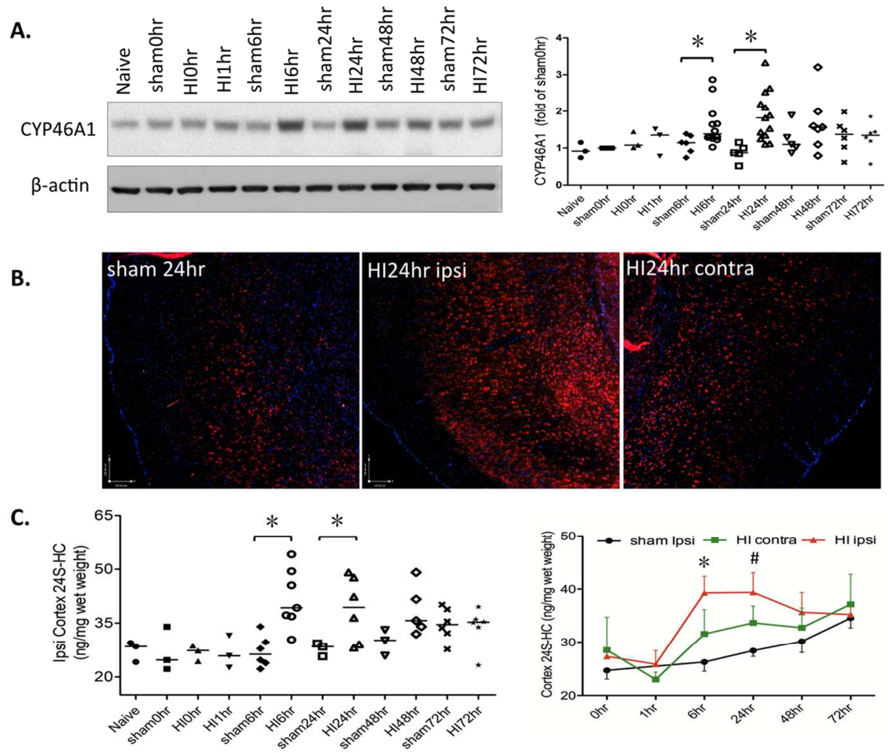

Figure 1: Up-regulation of CYP46A1 with a concomitant increase of 24S-HC in the ipsilateral cortex after neonatal HI. A. Protein expression of CYP46A1 in the sham-operated and HI-injured cortices was measured by western blotting at the indicated time points and presented as the OD ratio to β-actin and normalized to the values of sham 0hr (graph on the right, sham vs. HI: * p= 0.0339 at 6hr; * p=0.0026 at 24hr; n=5-6 for sham animals, n=6-12 for HI animals at 6-72hr). B. Immunofluorescent staining with anti-CYP46A1 antibody at 24hr after HI showed enhanced expression in the ipsilateral cortex than that in the contralateral side and in the sham animals. C. Increased production of 24S-HC (ng/mg tissue wet weight) in the ipsilateral cortex at 6hr and 24hr after HI (sham vs. HI: *p= 0.0167 at 6hr; *p=0.0085 at 24hr; n=3-6 for sham animals, n=5-7 for HI animals at 6-72hr). The time course of the changes in 24S-HC in the sham-, contra- and ipsilateral cortex is shown on the right. At 6hr, 24S-HC in the ipsilateral cortex was higher than that in the contralateral side (ipsi- vs. contra-: *p=0.0493). #: Significant difference between the ipsi- and the sham animals only, but not between the ipsi- and contralateral hemisphere.

121x91mm (300 x 300 DPI)

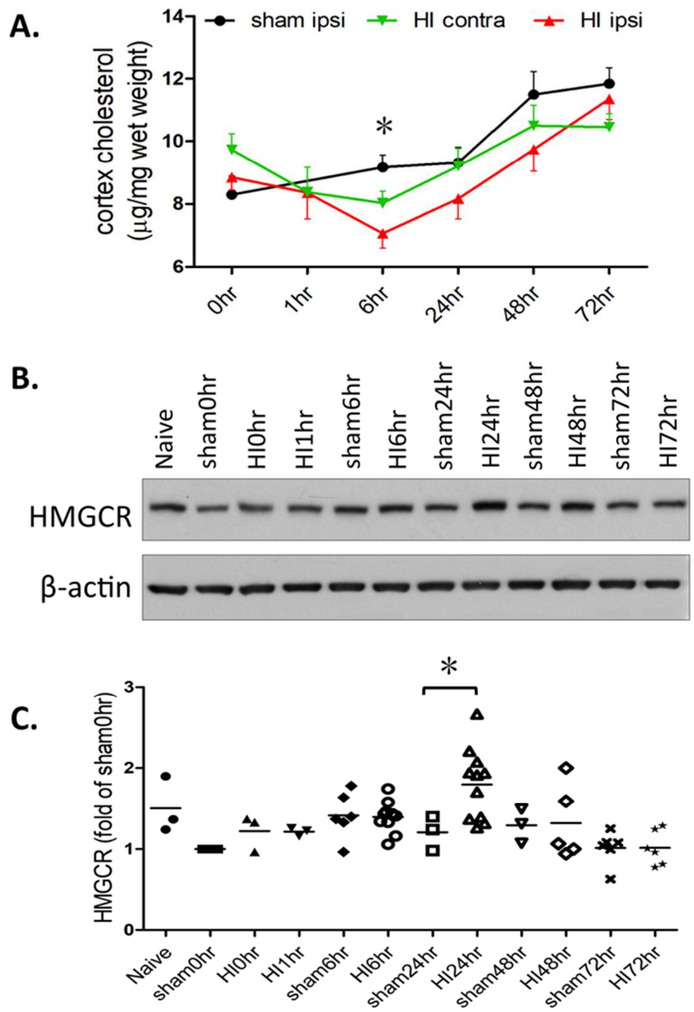

Figure 2: Transient cholesterol loss at 6hr after neonatal HI. A. The time course of the changes in cholesterol amount in the sham-, contra- and ipsilateral cortex following neonatal HI (sham vs. HI: * p=0.0304 at 6hr; n=4-7 for each time points). B. Protein expression of HMGCR in the sham and HI-injured cortices was measured by western blotting at the indicated time points. C. HMGCR expression is presented as the OD ratio to β-actin and normalized to the values of sham 0hr (sham vs. HI: *p=0.047 at 24hr, n=4-11).

85x91mm (300 x 300 DPI)

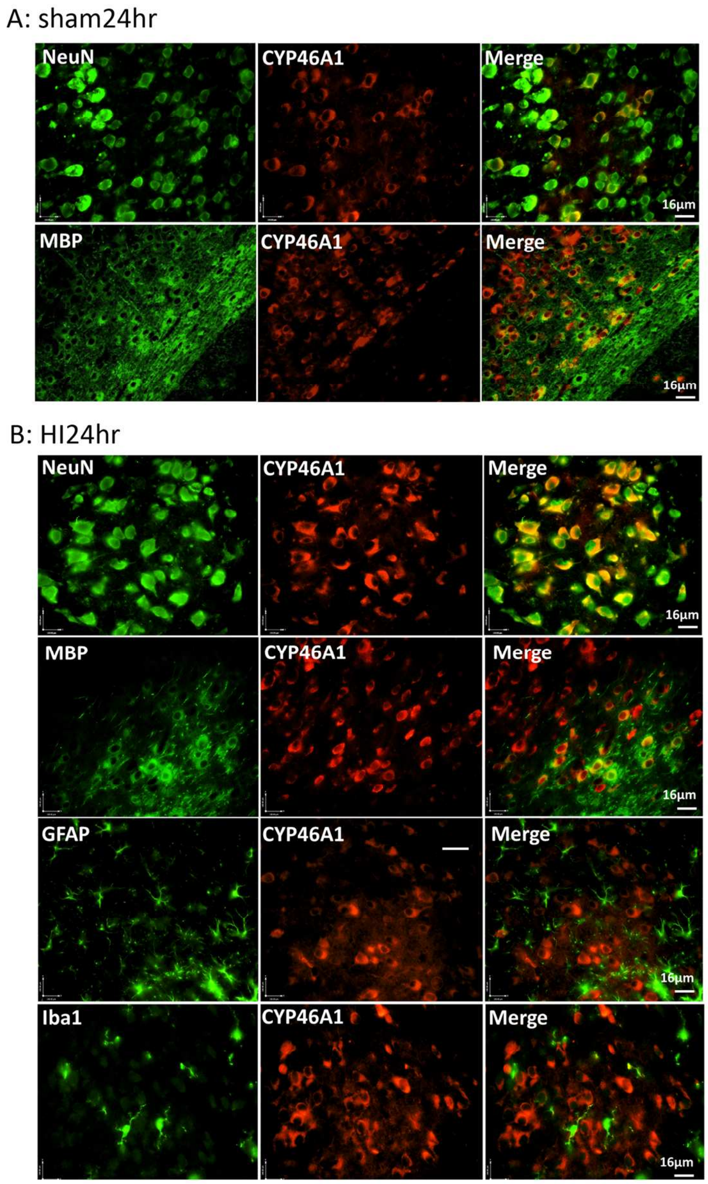

Figure 3: Expression of CYP46A1 in the neurons and oligodendrocytes. Images of double Immunofluorescent staining with CYP46A1 antibody (red, middle panels) paired with another antibody specific for neuron (NeuN), oligodendrocyte (MBP), astrocyte (GFAP), or microglia (Iba1), shown in green on the left panels. The representative images from the sham (A) and HI-injured animals at 24hr after HI (B).

135x211mm (300 x 300 DPI)

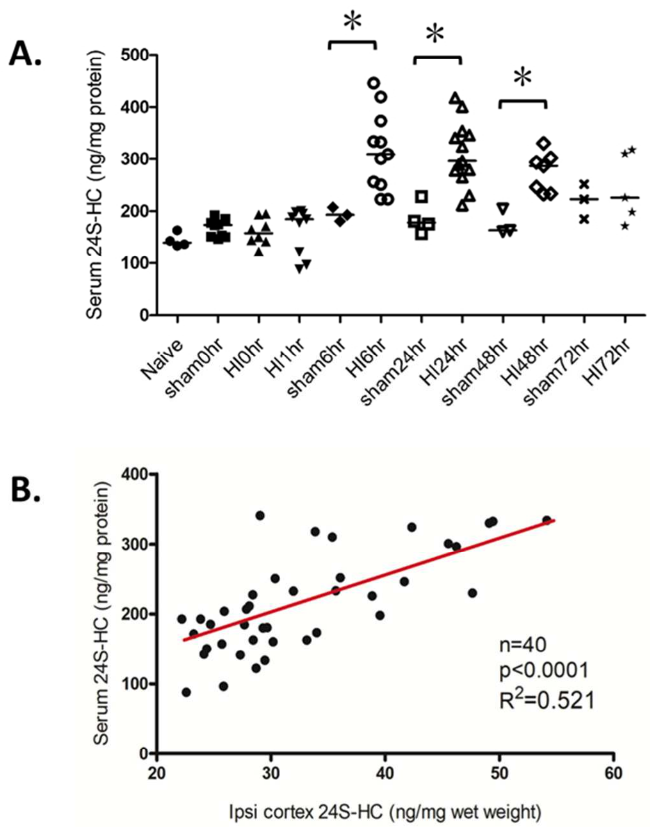

Figure 4: Correlation of the 24S-HC levels in the serum and in the ipsilateral cortex after neonatal HI. A. Quantification of the serum levels of 24S-HC (ng/mg serum protein) at the indicated post-HI time points. Sham vs. HI, *p=0.0102 at 6hr; *p=0.0046 at 24hr; *p=0.0167 at 48hr; n=4-6 for sham animals, n=5-13 for HI animals at 6-72hr. B. Correlation of 24S-HC levels in the serum and in the ipsilateral cortex. The samples used in Pearson's correlation coefficient analysis were those included in Fig. 1C. (n = 40, R2=0.521, p< 0.0001).

77x91mm (300 x 300 DPI)

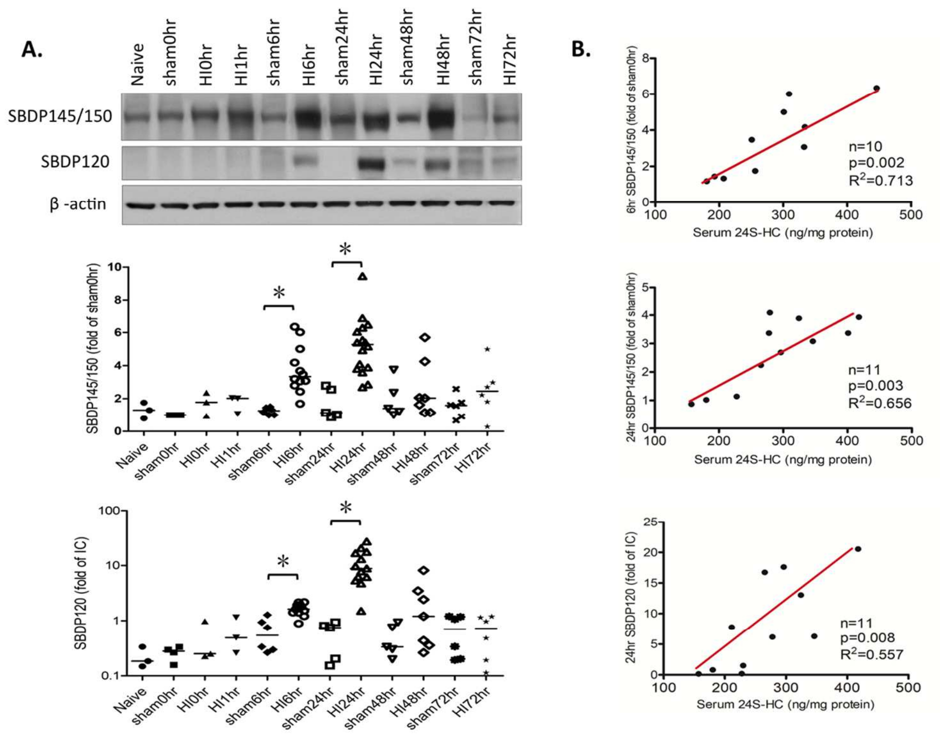

Figure 5: Correlation of the serum levels of 24S-HC with the expression of spectrin breakdown products (SBDP) at 6hr and 24hr after neonatal HI. A. Protein expression of SBDP145/150KD and SBDP120KD in the sham and HI-injured cortices was measured by western blotting at the indicated time points and presented as the OD ratio to β-actin and normalized to the values of sham 0hr (for SBDP145/150), or an internal control (IC, for SBDP120). For SBDP145/150KD, sham vs. HI, $*p=0.0094$ at 6hr, $*p=0.0013$ at 24hr. For SBDP120KD, sham vs. HI, $*p=0.036$ at 6hr, $*p=0.0087$ at 24hr. (n=4-6 for sham animals, n=6-15 for HI animals from 6-72hr). B. Correlation of serum 24S-HC with the expression of SBDP145/150KD at 6hr (top), at 24hr (middle), and with the expression of SBDP120KD at 24hr (bottom). Sample number, R2 and p values are shown in the graphs.

121x91mm (300 x 300 DPI)

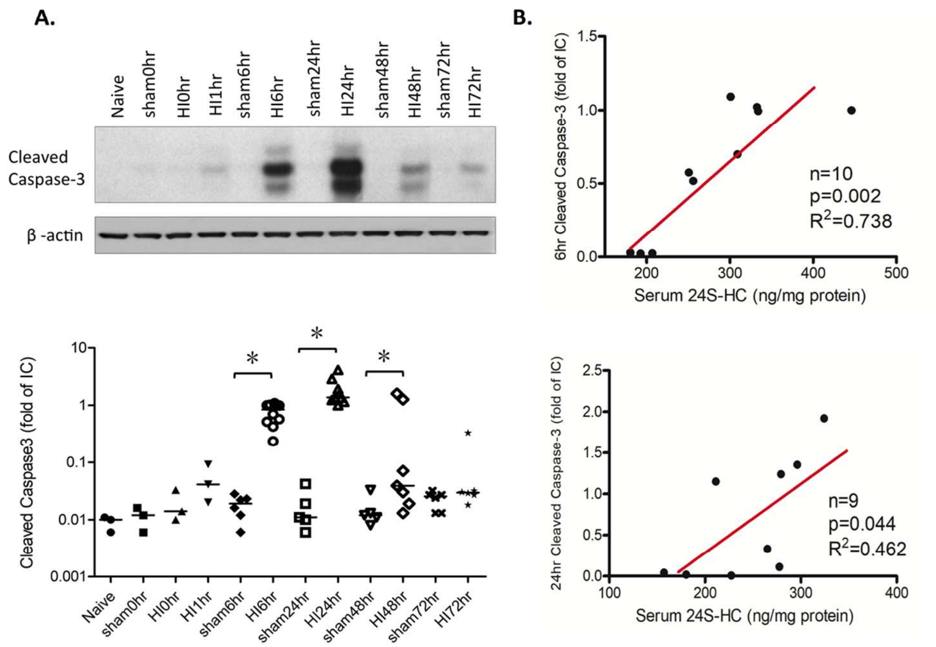

Figure 6: Correlation of the serum levels of 24S-HC with the expression of cleaved caspase-3 at 6hr and 24hr after neonatal HI. A. Protein expression of cleaved caspase-3 in the sham and HI-injured cortices was measured by western blotting at the indicated time points and presented as the OD ratio to β-actin and normalized to an internal control (IC). Sham vs. HI, *p=0.0112 at 6hr; *p=0.0027 at 24hr; *p=0.0228 at 72hr (n=5-6 for sham animals, n=7-10 for HI animals from 6-72hr). B. Correlation of serum 24S-HC with the expression of cleaved caspase-3 at 6hr (top) and at 24hr (bottom). Sample number, R2 and p values are shown in the graphs.

121x91mm (300 x 300 DPI)